Biochemical and Biophysical Research Communications 399 (2010) 42–48

Contents lists available at ScienceDirect

Biochemical and Biophysical Research Communications

journal homepage: www.elsevier.com/locate/ybbrc

Transplantation of marrow-derived cardiac stem cells carried in designer self-assembling peptide nanofibers improves cardiac function after myocardial infarction

Hai-dong Guo [a], Guo-hong Cui [b], Hai-jie Wang [a], Yu-zhen Tan [a,*]

[a] Department of Anatomy and Histology and Embryology, Shanghai Medical School of Fudan University, 138 Yixueyuan Road, Shanghai 200032, China
[b] Department of Neurology, Ruijin Hospital affiliated to School of Medicine, Shanghai Jiaotong University, Shanghai 200025, China

ARTICLE INFO

Article history:
Received 5 July 2010
Available online 15 July 2010

Keywords:
Myocardial infarction
Stem cell
Transplantation
Self-assembling peptide

ABSTRACT

Progress in stem cell transplantation for the treatment of myocardial infarction is hampered by the poor retention and survival of the implanted cells. To enhance cell survival and differentiation and thereby improve the efficiency of stem cell therapy, we constructed a novel self-assembling peptide by attaching an RGDSP cell-adhesion motif to the self-assembling peptide RADA16. c-kit^{pos}/Nkx2.5^{low}/GATA4^{low} marrow-derived cardiac stem cells (MCSCs), which have a specific potential to differentiate into cardiomyocytes, were isolated from rat bone marrow. The cytoprotective effects of RGDSP scaffolds were assessed by exposure of MCSCs to anoxia *in vitro*. The efficacy of transplanting MCSCs in RGDSP scaffolds was evaluated in a female rat MI model. The designer self-assembling peptide self-assembled into RGDSP nanofiber scaffolds under physiological conditions. RGDSP scaffolds were beneficial for the growth of MCSCs and protected them from apoptosis and necrosis caused by anoxia. In a rat MI model, cardiac function was improved and collagen deposition was markedly reduced in the group receiving MCSCs in RGDSP scaffolds compared with groups receiving MCSCs alone, RGDSP scaffolds alone or MCSCs in RADA16 scaffolds. There were more surviving MCSCs in the group receiving MCSCs in RGDSP scaffolds than in the groups receiving MCSCs alone or MCSCs in RADA16 scaffolds. Most of the Y chromosome-positive cells expressed cardiac troponin T and connexin43 (Cx-43). These results suggest that RGDSP scaffolds provide a suitable microenvironment for the survival and differentiation of MCSCs. RGDSP scaffolds enhanced the efficacy of MCSC transplantation to repair myocardium and improve cardiac function.

1. Introduction

Myocardial infarction is a major health problem and the leading cause of death and disability in both industrialized and developing nations. After a myocardial infarction, injured cardiomyocytes are gradually replaced by fibrous tissue, which may lead to heart failure [1,2]. Stem cell therapy is a promising therapeutic strategy for treating myocardial infarction [3–8]. Transplanted cells have been widely reported to engraft into the host myocardium, but with variability in the degree of differentiation. We have isolated marrow-derived cardiac stem cells (MCSCs) from rat mesenchymal stem cells (MSCs) by single-cell cloning culture and their expression of c-kit, Nkx2.5 and GATA4 [9]. Because MCSCs have a specific potential to differentiate into cardiomyocytes, MCSCs may be used as a good source of stem cells for stem cell transplantation in myocardial infarction.

Despite encouraging data from preclinical as well as clinical studies suggesting that stem cell therapy is a potential treatment for MI, the efficacy of the procedure remains hampered by the poor retention and survival of donor cells [10–16]. Attempts have been made to incorporate cells into biomaterials that might provide a fine-tuned, three-dimensional environment facilitating cell survival, proliferation and differentiation. Self-assembling peptide nanofiber scaffolds with more than 99% water content have been shown to be a good biological material for cell culture and tissue regeneration. The self-assembling peptide nanofiber microenvironment has been shown to promote the organization and survival of many different cell types, including cardiomyocytes [17] and endothelial cells [18]. Furthermore, self-assembling peptides can be engineered for protein delivery [17,19,20].

Recently, a class of designer self-assembling peptide scaffolds has been directly functionalized with short functional sequences via solid-phase synthesis extension at the C-terminus. The designer peptide scaffolds significantly enhanced adult mouse neural stem cell survival, proliferation, and differentiation into neurons and glial cells [21]. Biological designer self-assembling peptide nanofiber

* Corresponding author. Fax: +86 21 54237430.
E-mail address: yztan8@yahoo.com.cn (Y.-Z. Tan).

0006-291X/$ - see front matter © 2010 Elsevier Inc. All rights reserved.
doi:10.1016/j.bbrc.2010.07.031

scaffolds significantly enhance osteoblast proliferation, differentiation and three-dimensional migration [22]. However, the modification of self-assembling peptides with bioactive peptides to facilitate the adhesion and survival of stem cells, to promote the differentiation of stem cells towards cardiomyocytes, and to improve the effects of stem cell transplantation for the treatment of MI, has not been reported. In this study, we designed and synthesized a novel self-assembling peptide that not only facilitates the adhesion of MCSCs, but also promotes the differentiation of MCSCs towards cardiomyocytes. The efficacy of MCSC transplantation in RGDSP scaffolds was evaluated in a female rat MI model.

2. Materials and methods

2.1. MCSC isolation and culture

MSCs were isolated from marrow from the femurs and tibiae of male Sprague–Dawley (SD) rats. Single-cell cloning culture was performed to select MCSCs using methods described previously [9,23]. The immunostaining of c-kit (Santa Cruz, USA) and RT-PCR analysis of the early cardiac transcription factors Nkx2.5 and GATA-4 were performed to identify MCSCs.

2.2. Designer peptide synthesis and atomic force microscopy (AFM)

To promote the adhesion, survival and differentiation of MCSCs, we modified the self-assembling peptide AcN-RADARADARADA-RADA-$CONH_2$ (RADA16) with a functional RGDSP peptide motif to design a novel self-assembling peptide (RGDSP). RGDSP is an adhesion sequence, and it can promote cell adhesion and stimulate integrins relevant to early cardiac development [24]. The designer peptide RGDSP and RADA16 were custom-synthesized. They were dissolved in distilled sterile water (GIBCO, USA) at a final concentration of 1% (w/v) (10 mg/ml) and sonicated for 30 min before use. The structures of the peptides were observed under AFM using the method described by Horii et al. [22].

2.3. MCSCs seeding in RGDSP scaffolds

For MCSC seeding in nanofiber scaffolds, 30 μl of RADA16 or RGDSP solution was added to evenly cover the bottom surface of each well of a 96-well plate (BD Biosciences), followed by the slow addition of 200 μl/well of basal medium containing MCSCs at a density of 2.5×10^5 cells/ml. The cells seeded in scaffolds were cultured at 37 °C in a humidified atmosphere containing 5% CO_2.

2.4. Cytoprotective effects of RGDSP scaffolds against oxygen and glucose deprivation

To detect the cytoprotective effects of RGDSP scaffolds for MCSCs, the oxygen and glucose deprivation (OGD) model was established *in vitro*. After culturing for 24 h in 96-well culture plates, the cell culture medium from groups of MCSCs, MCSCs in RADA16 and MCSCs in RGDSP was replaced with glucose and serum-free DMEM (Gibco, USA). Then, the plates were placed in a 37 °C anoxia chamber saturated with 95% N_2/5% CO_2. The chamber was made according to the method used by Hori [25]. At 12 h after incubation, the cells from each group were stained with acridine orange/ethidium bromide (AO/EB). Both AO and EB were dissolved in 0.01 M PBS at a concentration of 100 μg/ml. The fluorescent dyes AO and EB were added to the supernatant. Digital images were acquired, and the number of differentially stained cells in random fields of 500 cells was determined. The data are expressed as the percentage of live, apoptotic and necrotic cells.

2.5. Myocardial infarction model and MCSC transplantation

Female SD rats (200–250 g) were anesthetized with 10% chloral hydrate (0.4 ml/100 g). Myocardial infraction was performed as described by Davis et al. [17]. Thirty minutes later, the rats were randomly divided into control, MCSC alone, RADA16 alone, MCSCs in RADA16, RGDSP alone and MCSCs in RGDSP groups. In the MCSCs in RADA16 and RGDSP groups, RADA16 and RGDSP were dissolved in sterile sucrose (295 mmol/l) at 1% (w/v) and sonicated for 10 min. A total of 5×10^6 MCSCs were suspended in 80 μl of the peptide solution. Immediately following suspension, the solution was injected into the border of the infarcted myocardium through a 30-gauge needle while the heart was beating. PBS (80 μl), or 5×10^6 MCSCs in 80 μl PBS, or RADA16 (80 μl), or RGDSP (80 μl) was injected into the control, MCSCs alone, RADA16 alone or RGDSP alone rats, respectively. The injection was administered at four points with 20 μl for each point.

2.6. Echocardiography

In order to evaluate the recovery of cardiac function, transthoracic echocardiography was performed at 4 weeks after transplantation. Care was taken to avoid excessive pressure on the thorax, which could induce bradycardia. After adequate two-dimensional images were obtained, the M-mode cursor was positioned to the parasternal long axis view at the papillary muscle level. LV internal dimensions and LV end-systolic (LVESD) and end-diastolic (LVEDD) diameters were measured from at least three consecutive cardiac cycles. Ejection fraction (EF) and fractional shortening (FS) as measures of systolic function were calculated using the equations $EF = [(LVEDD^3 - LVESD^3)/LVEDD^3] \times 100$ and $FS = (LVEDD - LVESD)/LVEDD \times 100$, respectively. The EF and FS results are expressed as percentages.

2.7. Histological examination

To detect fibrosis in cardiac muscle, the hearts were excised, cut transversely, embedded in paraffin and stained with Masson's trichrome. The blue area was regarded as fibrotic tissue. Five different ventricular slices covering the whole infarcted area from the apex to the site of occlusion were scanned and computerized with a digital image analyzer (ImagePro plus). The collagen volume fraction was calculated as the sum of all areas containing connective tissue divided by the total area of the image.

2.8. Reverse transcription polymerase chain reaction (RT-PCR)

Polymerase chain reaction (PCR) amplification was used to identify surviving transplanted male MCSCs via their Y chromosome. LV tissue from the injection site was isolated and refrigerated in liquid nitrogen. Genomic DNA was extracted for PCR template. Genomic DNA templates (100 ng) from different groups were used in PCR reactions (50 μl) with rat SRY primers according to the protocols published by Müller-Ehmsen et al. [26]. The intensities of the ethidium–bromide stained SRY bands were quantified using NIH Image (Wayne Rasband, NIH, USA) and subsequently normalized to β-actin mRNA levels.

2.9. Fluorescence in situ hybridization and immunohistochemical staining

For detecting the transplanted cells, *in situ* hybridization using a rat Y chromosome-specific gene was performed. Frozen sections were fixed with methanol and acetic acid (3:1) for 30 min at 4 °C, and then the slides were immersed in denaturation buffer (70%

formamide) at 95 °C for 5 min to denature the fixed chromosome specimens. After denaturation, the samples were dehydrated through a gradient ethanol series of 70%, 80%, 95% and 100% at –20 °C for 5 min each and then air-dried. The biotin labeled Y chromosome-specific probe (Roche, Germany) was denatured at 95 °C for 5 min. The sections were incubated with the denatured probe at 42 °C overnight in a moist chamber. After washing twice with 2× saline sodium citrate buffer, the sections were incubated with streptavidin-FITC (BioLegend, USA) for 30 min at 37 °C in the dark. To determine the differentiation of transplanted cells into cardiomyocytes and the relationship between differentiated cells and host cardiomyocytes, immunohistochemistry for cardiac troponin T (cTnT) and connexin43 (Cx-43) was performed. The same sections were treated with blocking solution for 30 min at 37 °C and then incubated with mouse cTnT monoclonal antibody (1:300, Santa Cruz) or rabbit Cx-43 polyclonal antibody (1:200, Abcam, USA) at 4 °C overnight. The sections were incubated with donkey anti-mouse or goat anti-rabbit cy3-conjugated antibody (Jackson, USA) for 30 min at 37 °C. After washing, the nuclei were counterstained with DAPI (Molecular Probes, USA). The presence of the Y chromosome and cTnT or Cx-43 in the cells was determined under a fluorescence microscope.

2.10. Statistical analysis

The data are expressed as means ± standard deviation. To analyze the data statistically, we used Student's *t*-test and one-way analysis of variance (ANOVA) with Scheffe's *post hoc* multiple-comparison analysis. Values of $P < 0.05$ were considered to be statistically significant.

3. Results

3.1. Structure of the designer peptide

The self-assembling peptide RADA16 can undergo spontaneous assembly into well-ordered nanofibers in dilute aqueous conditions (Fig. 1A). AFM images revealed that the RGDSP peptide self-assembled into nanofibers ~10 nm in fiber diameter (Fig. 1B). Thus, the appended functional motif did not prevent peptide self-assembly.

3.2. Cytoprotective effects of RGDSP scaffolds against OGD

MCSCs showed a uniform fibroblast-like appearance and expressed c-kit (Supplementary Fig. S1A). The cells weakly expressed the early cardiac transcription factors Nkx2.5 and GATA-4 (Supplementary Fig. S1B). At 24 and 72 h after seeding, very few apoptotic and necrotic cells were observed in the RGDSP group according to AO/EB double staining. More cells in the RADA16 group underwent apoptosis at 72 h after seeding compared with the RGDSP group (Supplementary Fig. S2). After treatment with OGD, most MCSCs in the control group displayed apoptotic and necrotic morphological changes by AO/EB double staining. However, the number of apoptotic and necrotic cells was significantly lower in the RADA16 and RGDSP groups and the number of surviving cells was greater ($P < 0.01$) (Fig. 2A). Furthermore, there were more surviving cells in the RGDSP group than in the RADA16 group ($P < 0.01$), and the numbers of apoptotic cells and necrotic cells were both significantly less compared with the RADA16 group ($P < 0.01$) (Fig. 2B).

3.3. Improvement of LV contractile function

At 4 weeks after transplantation, EF and FS in the five treatment groups were improved more significantly than in the control group. The echocardiographic examination showed that EF and FS in the MCSC + RADA16 group (44.64 ± 4.21, 28.95 ± 3.25) were higher than in the RADA16 alone group (28.67 ± 5.14, 19.08 ± 3.30, $P < 0.01$) or the MCSC alone group (35.21 ± 3.79, 21.79 ± 4.85, $P < 0.01$). Compared with the MCSC alone group, the RGDSP alone group (31.23 ± 5.90, 19.97 ± 2.91, $P < 0.01$) and the MCSC + RADA16 group ($P < 0.01$), the EF and FS in the MCSC + RGDSP group (53.06 ± 5.26, 35.65 ± 2.16) were higher (Fig. 3A).

3.4. Myocardial fibrosis after transplantation

Masson's trichrome staining demonstrated obvious myocardial fibrosis in the control group. However, there was more regenerated myocardium in the infarction area in the MCSC alone group, the RADA16 alone group, the MCSC + RADA16 group, the RGDSP alone group and the MCSC + RGDSP at 4 weeks after transplantation. MCSC transplantation in RGDSP scaffolds significantly attenuated the development of myocardial fibrosis compared with the other groups (Fig. 3B). Quantitative analysis demonstrated that the collagen volume fraction in the MCSC + RGDSP group was significantly smaller than in the MCSC alone group, the RGDSP alone group or the MCSC + RADA16 group. Compared with the MCSC alone and RADA16 alone groups, the collagen content in the MCSC + RADA16 group was lower (Fig. 3C).

3.5. Survival of transplanted cells by PCR analysis

LV tissue from 10 rats in each group was used for detecting the SRY gene by PCR. All tissues from animal groups receiving MCSCs were positive, confirming the presence and survival of the transplanted cells, and all tissues from the control, RADA16 and RGDSP

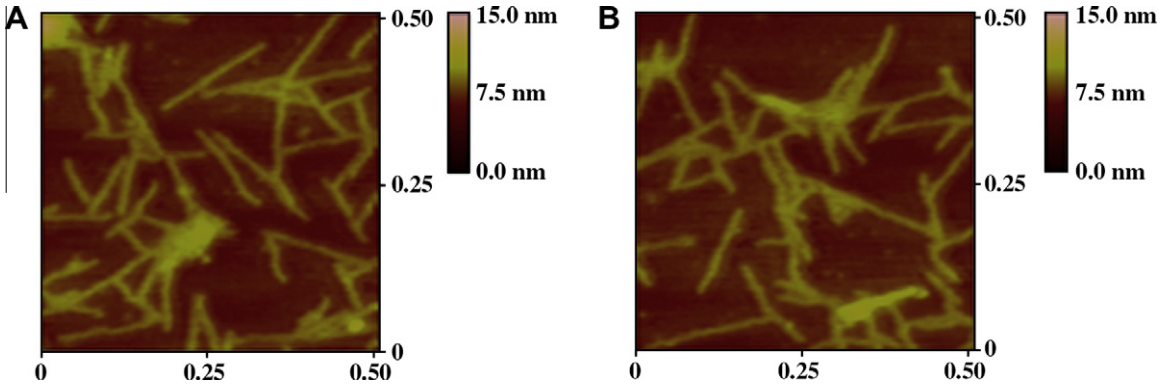

Fig. 1. Tapping mode AFM images of the peptides (A) RADA16 and (B) RGDSP. Both of the peptides self-assemble into nanofibers in water.

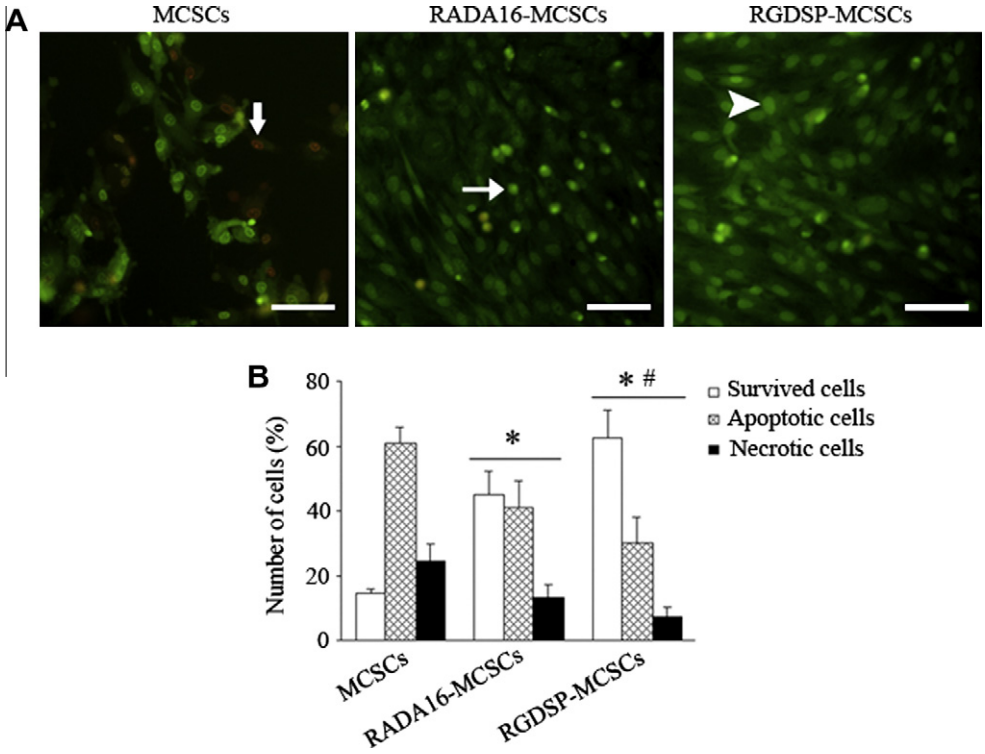

Fig. 2. Cytoprotection of MCSCs against OGD effects by RGDSP scaffolds. (A) AO/EB staining. Many cells underwent apoptosis and necrosis in the control group; however, most of the cells survived in the RADA16 and RGDSP groups. Scale bar: 50 μm. (B) Numbers of surviving, apoptotic and necrotic cells. $^{*}P < 0.01$ versus the control group. $^{\#}P < 0.01$ versus the RADA16 group; $n = 6$.

groups that did not receive MCSCs were negative (Fig. 4A). Quantitative analysis demonstrated that there were more surviving transplanted cells in the MCSC + RADA16 and MCSC + RGDSP groups than in the MCSC alone group. Between the MCSC + RGDSP group and the MCSC + RADA16 group, MCSC survival showed a significant difference (Fig. 4B).

3.6. Cardiomyogenic differentiation of donor cells in vivo

Y chromosome fluorescence *in situ* hybridization demonstrated that there were more Y chromosome-positive cells in the MCSC + RGDSP group than in the MCSC alone or MCSC + RADA16 groups at 4 weeks after transplantation, and most of the cells expressed cTnT and Cx-43. Cx-43 is located between Y chromosome-positive cells and recipient cardiomyocytes. The differentiated cells were aligned in parallel and connected with host cardiomyocytes (Fig. 4C and D).

4. Discussion

Our results showed that RADA16 scaffolds have good biocompatibility with MCSCs. Furthermore, when the cells were exposed to an OGD microenvironment, RADA16 scaffolds protected MCSCs against apoptosis and necrosis caused by the hostile conditions. Davis et al. reported that self-assembling peptides can create nanofiber microenvironments in the myocardium and that these microenvironments promote vascular cell recruitment [27]. The suitable microenvironment created by RADA16 promoted the survival and differentiation of MCSCs and eventually effectively improved heart function.

The modification of RADA16 has been intensely studied recently because designer self-assembling peptides modified with functional motifs have superior biological activities. In this study, we used an adhesion sequence (RGDSP) to directly extend the carboxyl terminus of the self-assembling peptide RADA16 and obtain designer self-assembling nanofibers. The addition of the RGDSP motif to the self-assembling peptide RADA16 did not inhibit its self-assembling properties or nanofiber formation. Most of the synthetic polymer biomaterials currently used in cell culture and regenerative medicine usually have microfiber structures [28,29]. However, RGDSP nanofibers, which have nanometer diameters, provide a three-dimensional microenvironment for the growth of MCSCs. The designer RGDSP scaffold may be useful not only for stem cell research, but also for future tissue regeneration.

We demonstrated that MCSC transplantation in RGDSP scaffolds decreased collagen deposition and improved heart function compared with the transplantation of MCSCs alone or MCSCs in RADA16. RGDSP scaffolds gave the cells a temporary three-dimensional nanofiber microenvironment after transplantation. Retention and adhesion are important conditions for the survival of transplanted cells and migration to the infarcted zone. The microenvironment provided by RGDSP scaffolds enhanced the survival and differentiation of MCSCs and played a key role in improving the efficiency of stem cell transplantation.

The three-dimensional space provided by RGDSP scaffolds and their functional motifs play a direct role in promoting the survival of MCSCs. MCSCs cultured in RGDSP scaffolds resisted apoptosis and necrosis induced by OGD treatment. The results of PCR for identifying the Y chromosome revealed that the survival of donor MCSCs was higher after injection in RGDSP scaffolds. In a two-dimensional environment, where only part of the cell body is in contact with the surface, receptor clustering at the attachment site may be induced; on the other hand, the receptors for growth factors, cytokines, nutrients and other signals are on the sides directly exposed to the culture medium. In the three-dimensional environment, the functional motifs on RGDSP scaffolds surround the whole cell body in all dimensions, and the factors may form a gradient in the three-dimensional nanoporous microenvironment. RGDSP

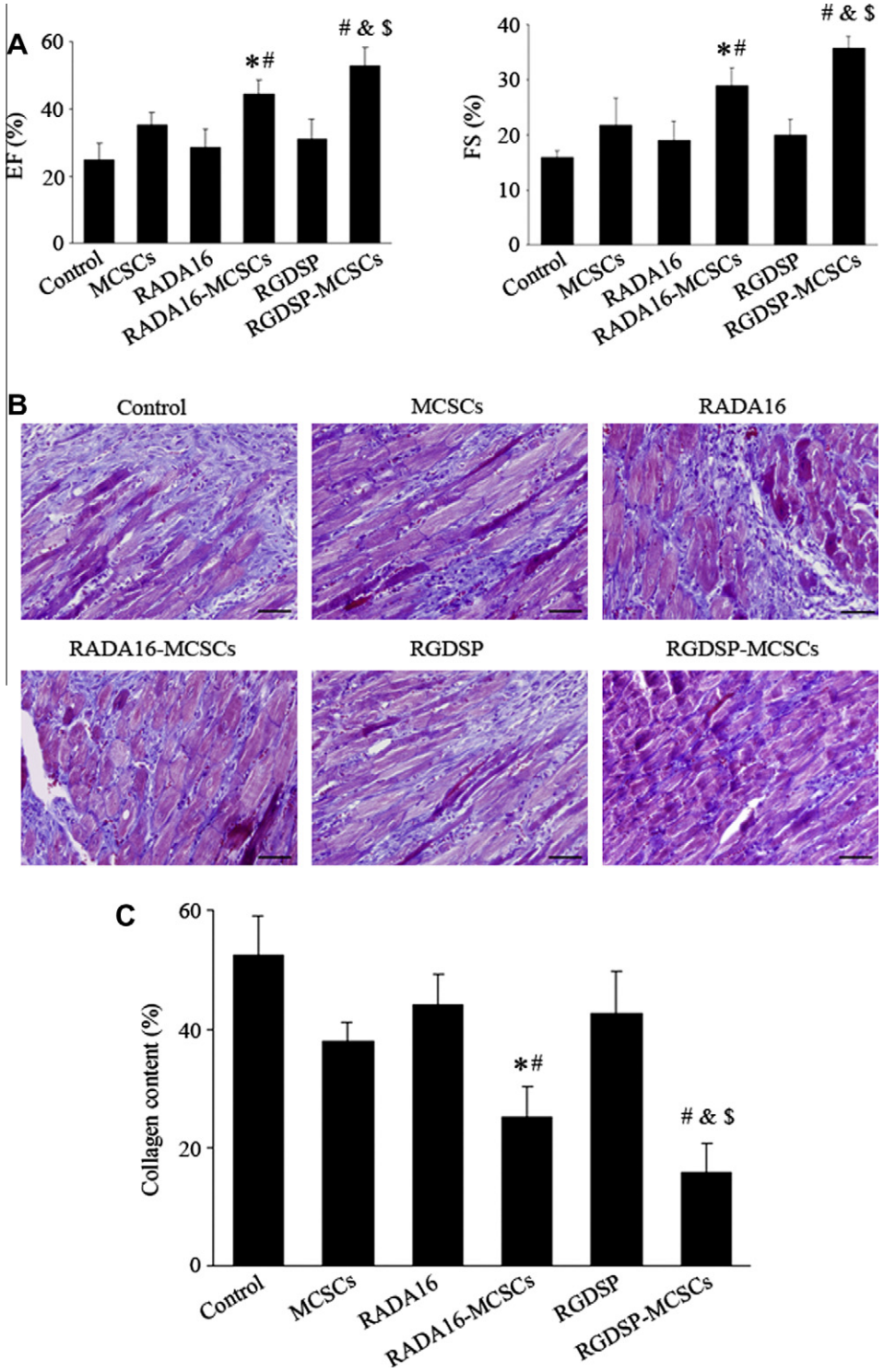

Fig. 3. Improvement of LV contractile function and collagen deposition at 4 weeks after transplantation. (A) EF (%) and FS (%) were compared among the different treatments. $^{*}P < 0.01$ versus the RADA16 group. $^{\#}P < 0.01$ versus the MCSC group. $^{\&}P < 0.01$ versus the RGDSP group. $^{\$}P < 0.01$ versus the MCSC + RADA16 group; $n = 10$. (B) Photomicrographs of representative myocardial sections stained with Masson's trichrome. Myocardium (red) was replaced significantly by fibrous tissue (blue) in the control group. Scale bar: 50 μm. (C) Quantitative analysis demonstrating that the collagen volume fraction in the MCSC + RGDSP group was significantly smaller than in the MCSC alone, RGDSP alone or MCSC + RADA16 groups. Compared with the MCSC alone and RADA16 alone groups, collagen content in the MCSC + RADA16 group was lower. $^{*}P < 0.01$ versus the RADA16 group. $^{\#}P < 0.01$ versus the MCSC group. $^{\&}P < 0.01$ versus the RGDSP group. $^{\$}P < 0.01$ versus the MCSC + RADA16 group; $n = 10$. (For interpretation of the references in color in this figure legend, the reader is referred to the web version of this article.)

scaffolds may also prevent anoikis by cell–matrix interactions *in vivo*. Anoikis is defined as programmed cell death induced by the loss of cell–matrix interactions [30]. Interactions between implanted MCSCs and RGDSP scaffolds may enhance the survival of donor cells by preventing anoikis.

The differentiation of transplanted stem cells into cardiomyocytes in the infarcted zone to replace the damaged recipient cardiomyocytes and improve heart function are the main objectives of stem cell transplantation. Although angiogenesis and paracrine action can improve cardiac function through indirect

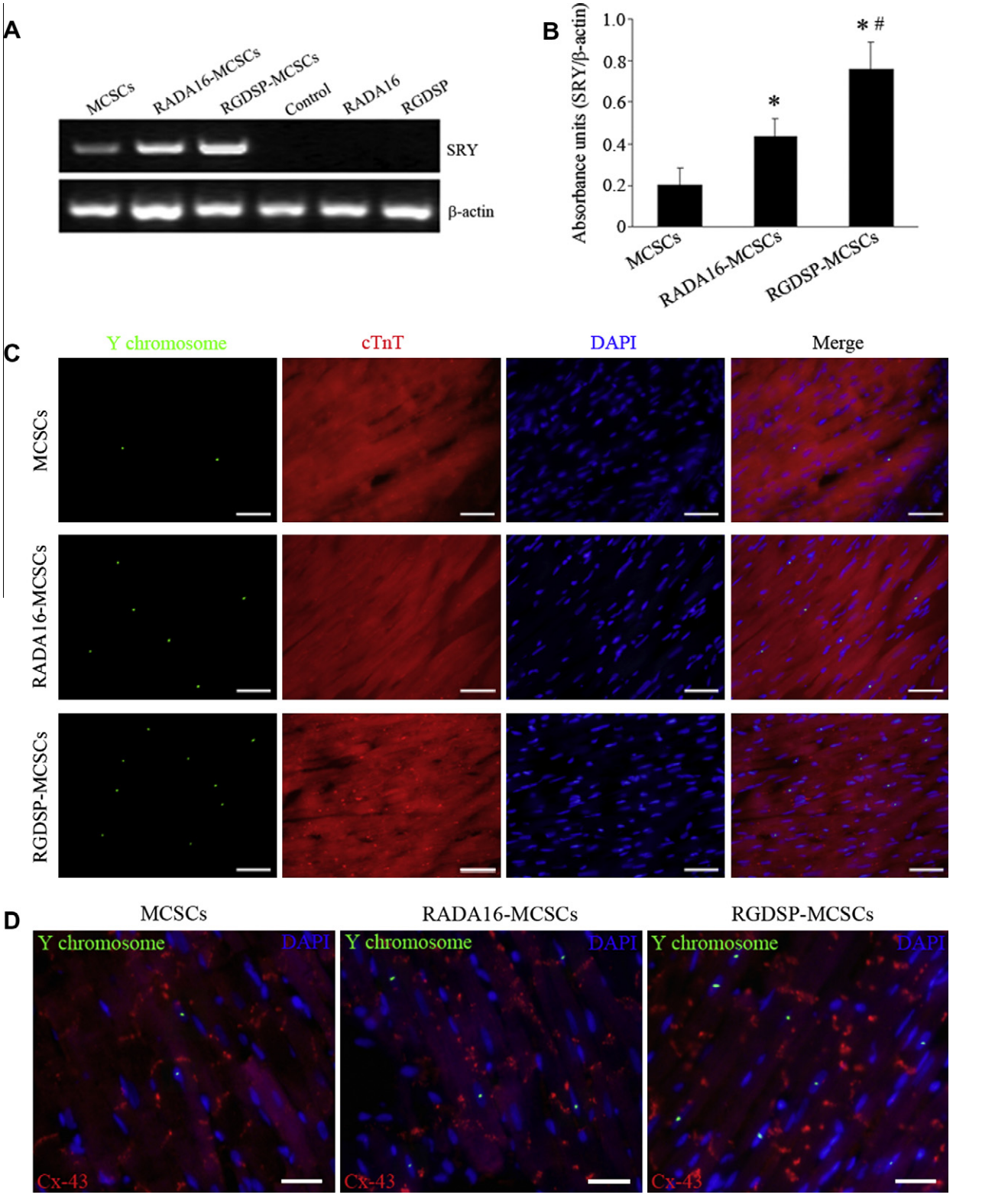

Fig. 4. Survival and cardiomyogenic differentiation of donor cells *in vivo*. (A) RT-PCR for the SRY gene using LV tissue from each group. (B) Quantitative analysis of SRY gene expression. $^{*}P < 0.01$ versus the MCSC alone group. $^{\#}P < 0.01$ versus in the MCSC + RADA16 group. (C) Expression of cTnT by Y chromosome-positive cells. Most Y chromosome-positive cells in the infarct and border zones co-expressed cTnT. Scale bar: 20 μm. (D) Expression of Cx-43 by Y chromosome-positive cells. Most of the transplanted cells expressed Cx-43. Cx-43 was located between Y chromosome-positive cells and recipient cardiomyocytes. The differentiated cells were aligned in parallel and connected with recipient cardiomyocytes. Scale bar: 25 μm.

effects, they can only save the dying cardiomyocytes or mobilize cardiac stem cells within the recipient heart. The number of cardiac stem cells produced by mobilization is few and the damaged cardiomyocytes cannot be replaced effectively. Quevedo et al. reported that allogeneic mesenchymal stem cells can reduce the infarcted area and improve cardiac function in chronic ischemic cardiomyopathy via their trilineage differentiation capacity, including cardiomyogenesis [31]. In our study, at 4 weeks after

transplantation, there were more donor cells expressing cTnT and Cx-43 in the MCSC + RGDSP scaffold group than in the MCSC alone or MCSC + RADA16 group. The engrafted cells underwent cardiomyogenic differentiation, formed mature muscle fibers and formed gap junctions with the myocardium of the recipient. The adhesion sequence RGDSP not only promotes cell adhesion, but also stimulates the integrins relevant to early cardiac development ($\alpha_5\beta_1$ and $\alpha_V\beta_3$). Therefore, RGDSP scaffolds efficiently promote the differentiation of MCSCs into cardiomyocytes. Further studies are necessary, however, to elucidate the contractile nature of the newly formed muscle fibers after connection with the myocardium of recipient.

5. Conclusion

We have developed a novel biomimetic designer self-assembling peptide scaffold to enhance the adhesion, survival and differentiation of MCSCs. MCSC transplantation in RGDSP scaffolds was more conducive to the survival and differentiation of the transplanted cells and thereby improved cardiac repair and cardiac function.

Acknowledgments

This work was supported by grants from the Ninth Graduate Innovation Foundation of FuDan University, the Natural Science Foundation of China (Nos. 30470883 and 30971674) and the Research Fund for the Doctoral Program of Higher Education of China (No. 200802460044).

Appendix A. Supplementary data

Supplementary data associated with this article can be found, in the online version, at doi:10.1016/j.bbrc.2010.07.031.

References

[1] W.S. Colucci, Molecular and cellular mechanisms of myocardial failure, Am. J. Cardiol. 80 (1997) 15L–25L.
[2] J.M. Pfeffer, M.A. Pfeffer, P.J. Fletcher, et al., Progressive ventricular remodeling in rat with myocardial infarction, Am. J. Physiol. 260 (1991) H1406–H1414.
[3] D. Orlic, J. Kajstura, S. Chimenti, et al., Bone marrow cells regenerate infarcted myocardium, Nature 410 (2001) 701–705.
[4] D. Orlic, J.M. Hill, A.E. Arai, Stem cells for myocardial regeneration, Circ. Res. 91 (2002) 1092–1102.
[5] T. Kofidis, J.L. De Bruin, G. Hoyt, et al., Myocardial restoration with embryonic stem cell bioartifical tissue transplantation, J. Heart Lung Transplant. 24 (2005) 737–744.
[6] J. Muller-Ehmsen, L.H. Kedes, R.H. Schwinger, et al., Cellular cardiomyoplasty – a novel approach to treat heart disease, Congest. Heart Fail 8 (2002) 220–227.
[7] M. Scorsin, A. Hagege, J.T. Vilquin, et al., Comparison of the effects of fetal cardiomyocyte and skeletal myoblast transplantation on postinfarction left ventricular function, J. Thorac. Cardiovasc. Surg. 119 (2000) 1169–1175.
[8] H.C. Ott, N. Bonaros, R. Marksteiner, et al., Combined transplantation of skeletal myoblasts and bone marrow stem cells for myocardial repair in rats, Eur. J. Cardiothorac. Surg. 25 (2004) 627–634.
[9] G.T. Zhang, Y.Z. Tan, H.J. Wang, et al., Effects of marrow-derived cardiac stem cell transplantation after myocardial infarction in rats, Zhong Hua Xin Xue Guan Bing Za Zhi 35 (2007) 940–944.
[10] C.J. Teng, J. Luo, R.C. Chiu, et al., Massive mechanical loss of microspheres with direct intramyocardial injection in the beating heart: implications for cellular cardiomyoplasty, J. Thorac. Cardiovasc. Surg. 132 (2006) 628–632.
[11] M. Zhang, D. Methot, V. Poppa, et al., Cardiomyocyte grafting for cardiac repair: graft cell death and anti-death strategies, J. Mol. Cell Cardiol. 33 (2001) 907–921.
[12] A. Maurel, K. Azarnoush, L. Sabbah, et al., Can cold or heat shock improve skeletal myoblast engraftment in infarcted myocardium?, Transplantation 80 (2005) 660–665
[13] K. Azarnoush, A. Maurel, L. Sebbah, et al., Enhancement of the functional benefits of skeletal myoblast transplantation by means of coadministration of hypoxia-inducible factor 1alpha, J. Thorac. Cardiovasc. Surg. 130 (2005) 173–179.
[14] C. Toma, M.F. Pittenger, K.S. Cahill, et al., Human mesenchymal stem cells differentiate to a cardiomyocyte phenotype in the adult murine heart, Circulation 105 (2002) 93–98.
[15] H. Reinecke, M. Zhang, T. Bartosek, et al., Survival integration, and differentiation of cardiomyocyte grafts: a study in normal and injured rat hearts, Circulation 100 (1999) 193–202.
[16] D.T. Cooke, E.G. Hoyt, R.C. Robbins, Overexpression of human Bcl-2 in syngeneic rat donor lungs preserves posttransplant function and reduces intragraft caspase activity and interleukin-1beta production, Transplantation 79 (2005) 762–767.
[17] M.E. Davis, P.C. Hsieh, T. Takahashi, et al., Local myocardial insulin-like growth factor 1 (IGF-1) delivery with biotinylated peptide nanofibers improves cell therapy for myocardial infarction, Proc. Natl. Acad. Sci. USA 103 (2006) 8155–8160.
[18] D.A. Narmoneva, O. Oni, A.L. Sieminski, et al., Self-assembling short oligopeptides and the promotion of angiogenesis, Biomaterials 26 (2005) 4837–4846.
[19] V.F. Segers, R.T. Lee, Local delivery of proteins and the use of self-assembling peptides, Drug Discov. Today 12 (2007) 561–568.
[20] P.C. Hsieh, C. MacGillivray, J. Gannon, et al., Local controlled intramyocardial delivery of platelet-derived growth factor improves postinfarction ventricular function without pulmonary toxicity, Circulation 114 (2006) 637–644.
[21] F. Gelain, D. Bottai, A. Vescovi, et al., Designer self-assembling peptide nanofiber scaffolds for adult mouse neural stem cells 3-dimensional cultures, PLoS One 1 (2006) e119.
[22] A. Horii, X. Wang, F. Gelain, et al., Biological designer self-assembling peptide nanofiber scaffolds significantly enhance osteoblast proliferation, differentiation and 3-D migration, PLoS One 2 (2007) e190.
[23] H. Scadova, G. Qin, D.H. Cha, et al., Clonally expanded novel multipotent stem cells from human bone marrow regenerate myocardium after myocardial infarction, J. Clin. Invest. 115 (2005) 326–338.
[24] T.P. Kraehenbuehl, P. Zammaretti, A.J. Van der Vlies, et al., Three-dimensional extracellular matrix-directed cardioprogenitor differentiation: systematic modulation of a synthetic cell-responsive PEG-hydrogel, Biomaterials 29 (2008) 2757–2766.
[25] O. Hori, M. Matsumoto, K. Kuwabara, et al., Exposure of astrocytes to hypoxia/reoxygenation enhances expression of glucose-regulated protein 78 facilitating astrocyte release of the neuroprotective cytokine interleukin 6, J. Neurochem. 66 (1996) 973–979.
[26] J. Müller-Ehmsen, P. Whittaker, R.A. Kloner, et al., Survival and development of neonatal rat cardiomyocytes transplanted into adult myocardium, J. Mol. Cell Cardiol. 34 (2002) 107–116.
[27] M.E. Davis, J.P.M. Motion, D.A. Narmoneva, et al., Injectable self-assembling peptide nanofibers create intramyocardial microenvironments for endothelial cells, Circulation 111 (2005) 442–450.
[28] S. Sarkar, G.Y. Lee, J.Y. Wong, et al., Development and characterization of a porous micro-patterned scaffold for vascular tissue engineering applications, Biomaterials 27 (2006) 4775–4782.
[29] K. Tuzlakoglu, C.M. Alves, J.F. Mano, et al., Production and characterization of chitosan fibers and 3-D fiber mesh scaffolds for tissue engineering applications, Macromol. Biosci. 4 (2004) 811–819.
[30] A.J. Bretland, J. Lawry, R.M. Sharrard, A study of death by anoikis in cultured epithelial cells, Cell Prolif. 34 (2001) 199–210.
[31] H.C. Quevedo, K.E. Hatzistergos, B.N. Oskouei, et al., Allogeneic mesenchymal stem cells restore cardiac function in chronic ischemic cardiomyopathy via trilineage differentiating capacity, Proc. Natl. Acad. Sci. USA 106 (2009) 14022–14027.